SUPPORTING INFORMATION

Protein Side-Chain Dynamics and Residual Conformational Entropy

Nikola Trbovic,[‡] Jae-Hyun Cho,[‡] Robert Abel,[†] Richard A. Friesner,[†]

Mark Rance,[§] and Arthur G. Palmer III[‡,*]

[‡]Department of Biochemistry and Molecular Biophysics, Columbia University

[†]Department of Chemistry, Columbia University

[§]Department of Molecular Genetics, Biochemistry and Microbiology, University of Cincinnati

[*]Corresponding Author. E-mail: agp6@columbia.edu

Table S1. Measured R_1 rates in s^{-1}

Res.	9.4 T	11.7 T	14.1 T	16.4 T
R27	1.79 ± 0.02	1.31 ± 0.02	1.00 ± 0.01	0.82 ± 0.01
R29	0.62 ± 0.04	0.60 ± 0.04	0.49 ± 0.02	0.43 ± 0.01
R31	0.53 ± 0.03	0.50 ± 0.04	0.40 ± 0.02	0.36 ± 0.01
R41	1.20 ± 0.05	1.06 ± 0.04	0.95 ± 0.03	0.74 ± 0.02
R46	1.88 ± 0.02	1.27 ± 0.02	0.94 ± 0.02	0.77 ± 0.01
R75	1.26 ± 0.06	0.99 ± 0.04	0.83 ± 0.03	0.66 ± 0.01
R88	1.04 ± 0.03	0.95 ± 0.06	0.85 ± 0.04	0.71 ± 0.02
R106	1.77 ± 0.02	1.27 ± 0.01	0.91 ± 0.01	0.74 ± 0.01
R132	1.77 ± 0.03	1.42 ± 0.02	1.21 ± 0.03	0.97 ± 0.02
R138	1.37 ± 0.02	1.15 ± 0.01	0.94 ± 0.02	0.79 ± 0.01
X[a]	1.41 ± 0.02	1.06 ± 0.06	0.86 ± 0.04	0.85 ± 0.02

[a] Unassigned resonance near that of R138

Table S2. Measured R_2 rates in s^{-1}

Res.	9.4 T	11.7 T	14.1 T a[a]	14.1 T b[b]
R27	7.16 ± 0.03	6.88 ± 0.11	7.17 ± 0.15	7.09 ± 0.06
R29	2.14 ± 0.10	2.18 ± 0.13	2.34 ± 0.17	2.17 ± 0.09
R31	1.81 ± 0.13	1.72 ± 0.10	1.96 ± 0.22	1.77 ± 0.12
R41	2.92 ± 0.02	2.80 ± 0.07	2.98 ± 0.13	2.91 ± 0.03
R46	9.71 ± 0.10	9.71 ± 0.12	10.22 ± 0.26	9.90 ± 0.12
R75	4.41 ± 0.04	4.30 ± 0.08	4.70 ± 0.26	4.41 ± 0.06
R88	2.92 ± 0.18	2.98 ± 0.41	3.18 ± 0.13	2.89 ± 0.12
R106	9.83 ± 0.08	9.59 ± 0.12	10.30 ± 0.25	10.29 ± 0.13
R132	4.93 ± 0.02	4.74 ± 0.06	5.04 ± 0.12	4.82 ± 0.06
R138	4.03 ± 0.02	3.77 ± 0.07	4.14 ± 0.10	3.90 ± 0.09
X	4.20 ± 0.06	4.17 ± 0.19	4.35 ± 0.10	4.46 ± 0.21

[a] First 14.1 T R_2 data set; [b] Second 14.1 T R_2 data set

Table S3. Measured NOE rates

Res.	9.4 T	11.7 T	14.1 T	16.4 T
R27	0.48 ± 0.01	0.47 ± 0.01	0.48 ± 0.01	0.50 ± 0.01
R29	−1.27 ± 0.01	−1.21 ± 0.03	−1.14 ± 0.01	−1.21 ± 0.02
R31	−1.63 ± 0.03	−1.50 ± 0.07	−1.41 ± 0.02	−1.54 ± 0.06
R41	−0.49 ± 0.01	−0.32 ± 0.01	−0.22 ± 0.01	−0.12 ± 0.01
R46	0.76 ± 0.01	0.82 ± 0.04	0.80 ± 0.01	0.79 ± 0.01
R75	−0.19 ± 0.01	−0.21 ± 0.01	−0.20 ± 0.01	−0.17 ± 0.01
R88	−0.76 ± 0.02	−0.57 ± 0.02	−0.46 ± 0.04	−0.38 ± 0.01
R106	0.70 ± 0.01	0.71 ± 0.01	0.72 ± 0.02	0.73 ± 0.02
R132	0.14 ± 0.01	0.24 ± 0.01	0.30 ± 0.01	0.35 ± 0.01
R138	−0.15 ± 0.01	−0.14 ± 0.01	−0.04 ± 0.01	0.01 ± 0.02
X	−0.24 ± 0.06	−0.06 ± 0.04	−0.05 ± 0.02	0.05 ± 0.02

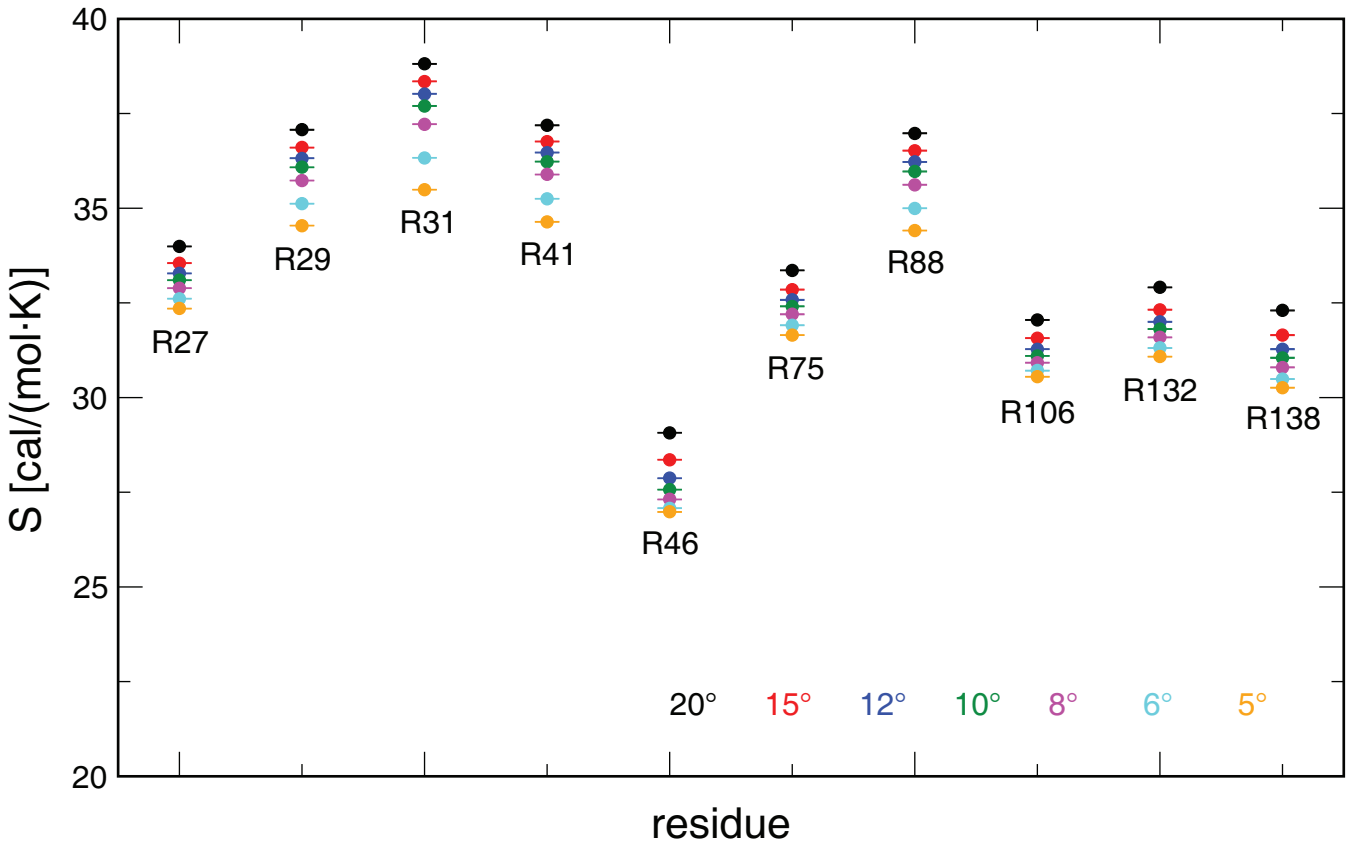

Figure S1. Dependence of simulated entropies on integration bin size. Bootstrap standard errors are shown.

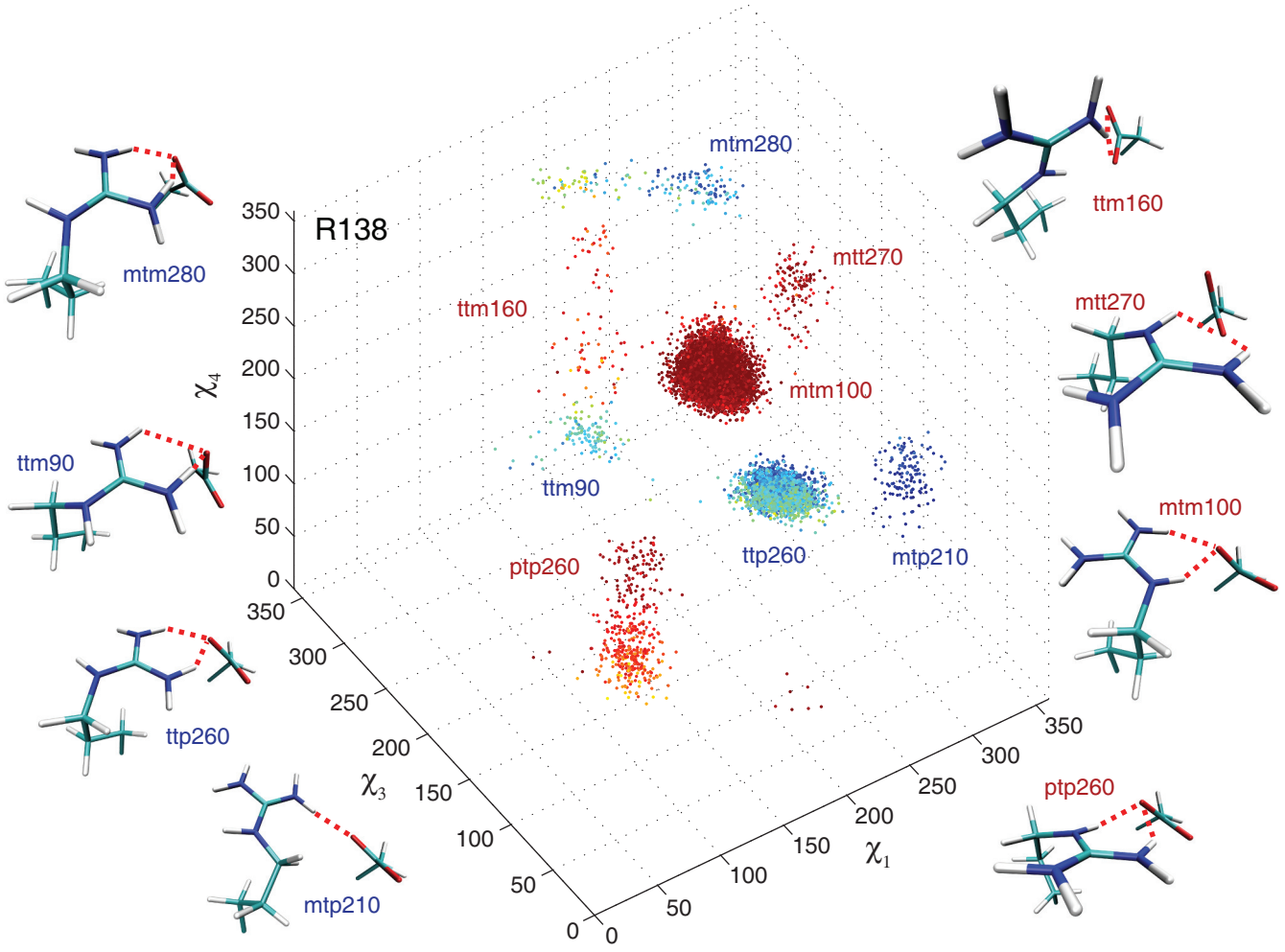

Figure S2. Three-dimensional χ-angle plot for R138. Every 10th conformation forming the salt bridge to D134 from all eight 20 ns trajectories is shown. Conformations are color-coded as in figure 5. The salt-bridge configuration of each conformation is indicated by the color of the corresponding rotamer label: red conformers form a salt bridge to D134 through the N$^{\eta}$ that is closer to N$^{\varepsilon}$, with the N$^{\varepsilon}$ partly involved - structures are shown on the right; blue conformers form this salt bridge through the N$^{\eta}$s, with the N$^{\varepsilon}$-H$^{\varepsilon}$ bond pointing away - structures are shown on the left. Salt bridges are indicated by red dashed lines.

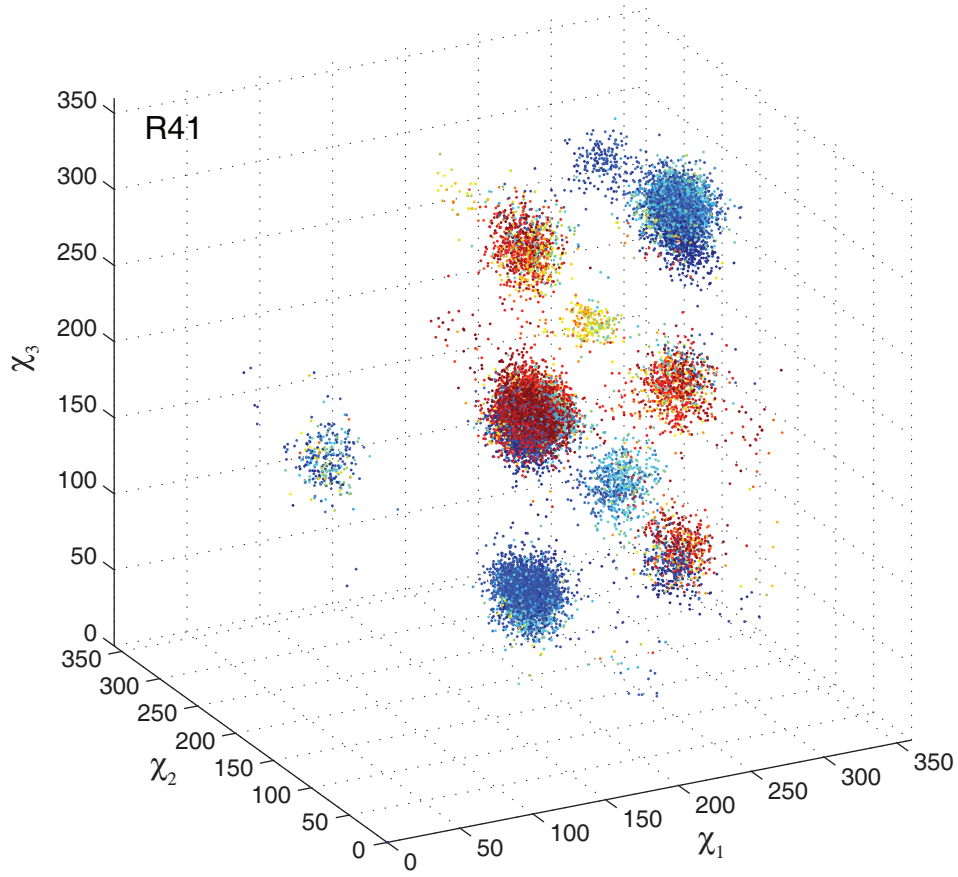

Figure S3. Three-dimensional χ-angle plot for R41. Every 10th conformation from all eight 20 ns trajectories is shown. Conformations are color-coded as in figure 5. The presence of multiple N^{ε}-H^{ε} bond-vector orientations within individual χ_1-χ_2-χ_3-conformers reflects additional disorder in χ_4.

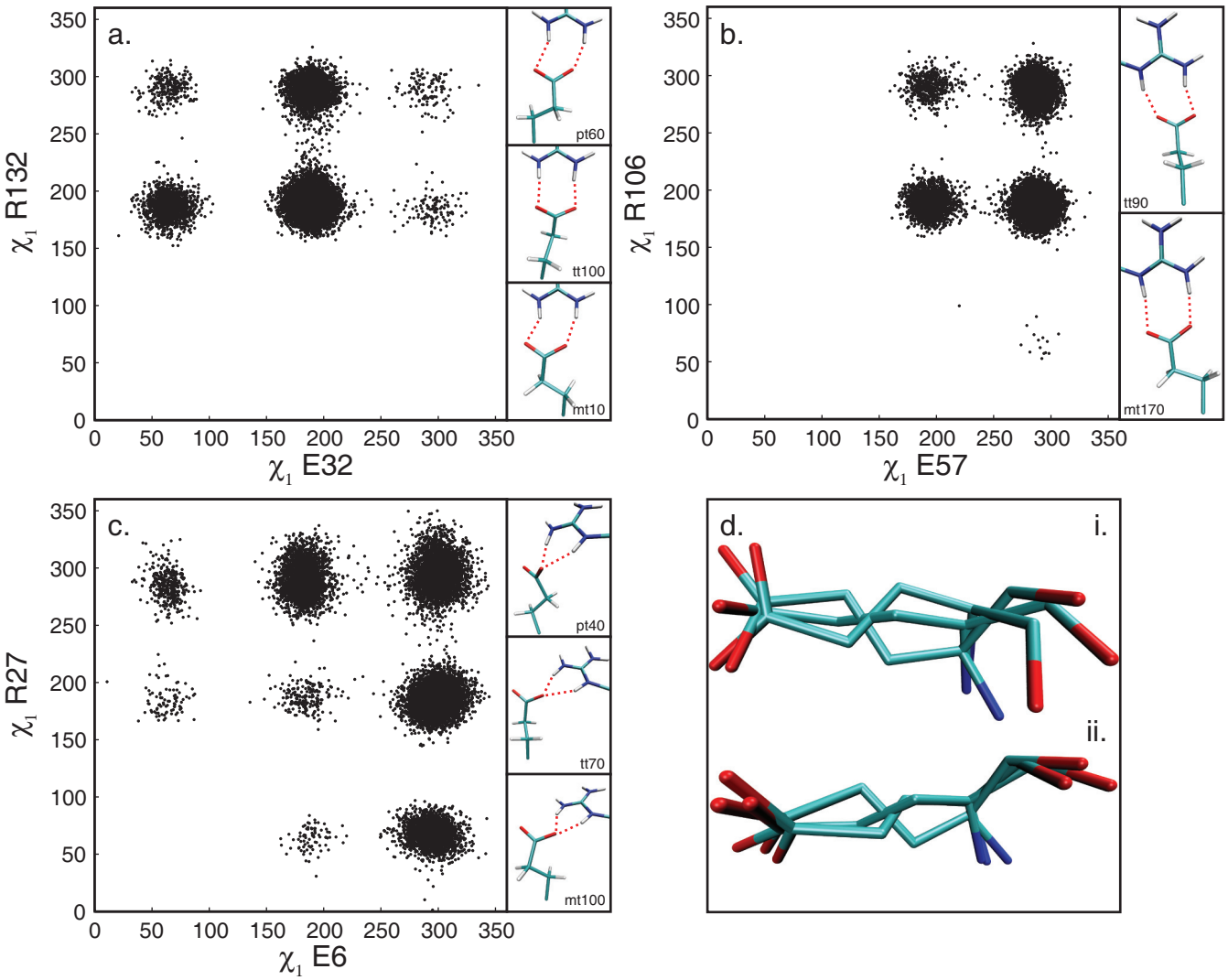

Figure S4. Dynamic decoupling in the glutamate side chain. (a-c) χ_1 of select glutamate residues vs. χ_1 of the respective salt-bridge partners. Every 10th conformation from all eight 20 ns trajectories is shown. For all three glutamates χ_2 is predominantly in the t rotamer. Representative structures including only the functional group of the respective salt-bridge partner are shown. (d) Group of glutamate rotamer-library conformations clustered according to C^{γ}-C^{δ} bond-vector orientation after joint heavy-atom superposition: (i) original library structures and (ii) library structures with χ_3 angles set to the average values of the three corresponding conformations of E32, with χ_2 in the t rotamer. When χ_2 of a glutamate is in the t rotamer, χ_3 is largely unconstrained within a basin approximately 180° wide.

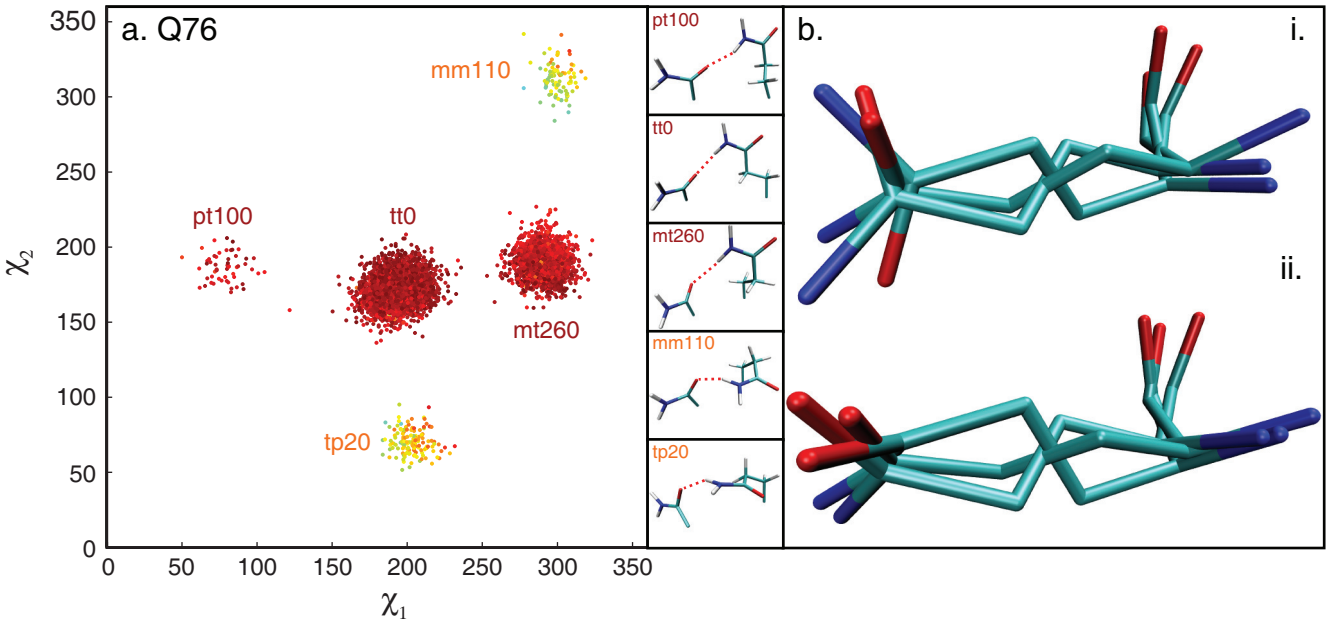

Figure S5. Dynamic decoupling in the glutamine side chain. (a) Two-dimensional χ-angle plot for Q76. Every 10th conformation forming the hydrogen bond to Q80 through H^{ε}_{22} from all eight 20 ns simulations is shown. Conformations are color-coded with respect to the scalar product of the orientation of the N^{ε}_{2}-H^{ε}_{22} bond vector and its orientation in the x-ray structure according to the color bar in figure 5. Although χ_2 is predominantly in the t rotamer, Q76 is to a small degree also able to form the hydrogen bond with its χ_2 in the p or m rotamers. This discrepancy with the analysis of the rotamer library is explained by deviations from ideal rotameric angles. Representative structures including only the functional group of the salt-bridge partner, Q80, are shown. (b) Group of glutamine rotamer-library conformations clustered according to C^{γ}-C^{δ} bond-vector orientation after joint heavy-atom superposition: (i) original library structures and (ii) library structures with χ_3 angles set to the average values of the three corresponding conformations of Q76, with χ_2 in the t rotamer. When χ_2 of a glutamine side chain is in the t rotamer, χ_3 is largely unconstrained within a basin approximately 180° wide.

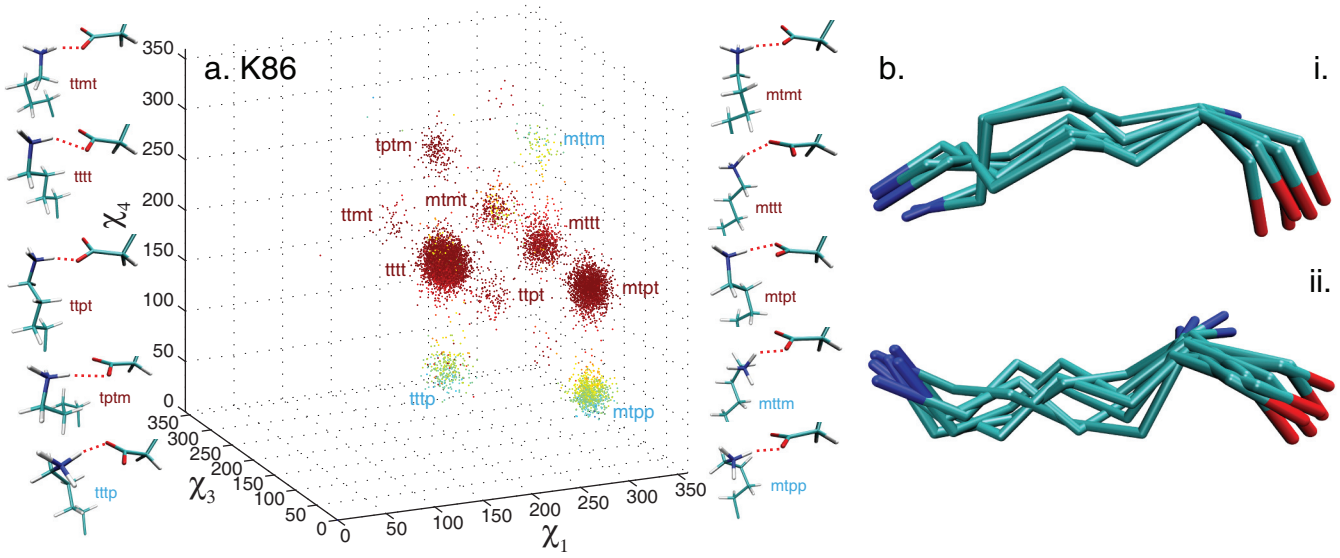

Figure S6. Dynamic decoupling in the lysine side chain. (a) Three-dimensional χ-angle plot for K86. Every 10th conformation forming the salt bridge to D108 from all eight 20 ns simulations is shown. Conformations are color-coded with respect to the scalar product of the orientation of the C^{ε}-N^{ζ} bond vector and its orientation in the first snapshot according to the color bar in figure 5. Representative structures are shown. (b) Two groups of lysine rotamer-library conformations clustered according to C^{ε}-N^{ζ} bond-vector orientation after joint heavy-atom superposition.

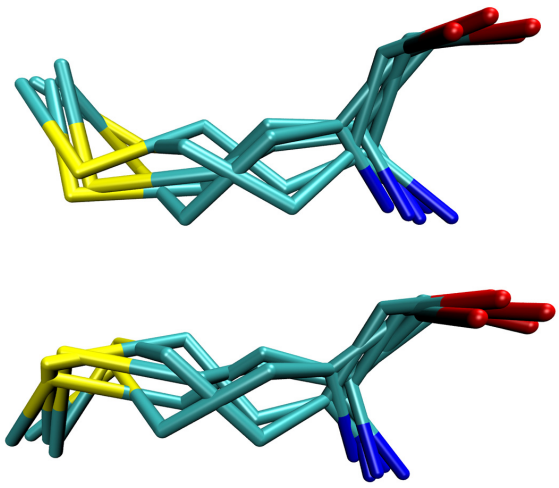

Figure S7. Two groups of methionine rotamer-library conformations clustered according to S^{δ}-C^{ε} bond-vector orientation after joint heavy-atom superposition.